ADVANCED BIOLOGY
www.advanced-bio.com

Tas1R3 Dependent and Independent Recognition of Sugars in the Urethra and the Role of Tuft Cells in this Process

*Patricia Schmidt, Alexander Perniss, Martin Bodenbenner-Tuerich, Silke Wiegand, Loic Briand, and Klaus Deckmann**

Increased sugar concentrations on mucosal surfaces display risk factors for infections. This study aims to clarify sugar monitoring in the urethra. Urethral tuft cells (UTC) are known sentinels monitoring the urethral lumen for potentially harmful substances and initiating protective mechanisms. Next-generation sequencing (NGS), RT-PCR, and immunohistochemistry show expression of the taste receptor Tas1R3 in murine UTC, a crucial component of the classical sweet detection pathway. Isolated UTC respond to various sugars with an increase of intracellular [Ca^{2+}]. The Tas1R3 inhibitor gurmarin and Tas1R3 deletion reduces these responses. Utilizing mice lacking UTC, glibenclamide, a K^+-ATP channel antagonist, and phlorizin, a SGLT1 inhibitor, reveal an additional Tas1R3 independent sweet detection pathway. Inhibition of both pathways abrogates the sugar responses. Rat cystometry shows that intraurethral application of sucrose and glucose increases detrusor muscle activity Tas1R3 dependently. Sugar monitoring in the urethra occurs via two distinct pathways. A Tas1R3 dependent pathway, exclusive to UTC, and a Tas1R3 independent sweet detection pathway, which can be found both in UTC and in other urethral epithelial cells.

P. Schmidt, A. Perniss, M. Bodenbenner-Tuerich, S. Wiegand, K. Deckmann
Institute for Anatomy and Cell Biology
Justus-Liebig-University Giessen
35385 Giessen, Germany
E-mail: Klaus.Deckmann@anatomie.med.uni-giessen.de

P. Schmidt
Leibniz Institute on Aging–Fritz Lipmann Institute
07745 Jena, Germany

A. Perniss
Division of Allergy and Clinical Immunology
Brigham and Women's Hospital and Department of Medicine
Harvard Medical School
Boston, MA 02115, USA

L. Briand
Centre des Sciences du Goût et de l'Alimentation
CNRS
INRAE
Institut Agro
Université de Bourgogne
Dijon F-21000, France

The ORCID identification number(s) for the author(s) of this article can be found under https://doi.org/10.1002/adbi.202400117

DOI: 10.1002/adbi.202400117

1. Introduction

Urinary tract infection (UTI) is one of the most common bacterial infections worldwide. Patients with diabetes mellitus (DM) are at higher risk for developing UTI´s, furthermore, the course of the disease is severe compared to non-diabetic patients prone to UTI´s.[1–9] Several mechanisms, specific to DM, may contribute to the increased risk of UTI.[8,9] An increase in the urine sugar concentration is ubiquitous in diabetic diseases and higher sugar concentrations in the urine promote the growth of pathogenic bacteria.[10–14] In the respiratory tract, glucose could be identified as a nutrient for bacteria[15] and diabetic patients are at increased risk of respiratory infection.[16] Accordingly, an elevated sugar concentration in the liquid film on mucosal surfaces is considered as an increased risk of infection.

The cellular mechanism of sugar detection is best characterized in type II sensory cells of the oropharyngeal taste bud. Here, a heterodimer of taste receptor type 1 member 3 and 2 (Tas1R3; Tas1R2) forms a sweet taste receptor[17,18] and downstream signaling occurs though taste-specific G protein α-gustducin (GNAT3), phospholipase Cβ2 (PLCβ2) and the transient potential receptor cation channel subfamily M (melanostatin) member 5 (TRPM5), all commonly known to be part of the canonical taste transduction cascade.[17,19,20] Mice lacking Tas1R3 show a reduced preference for sucrose and saccharin in behavioral assays.[21] Additionally, a Tas1R3 independent sweet detection pathway has been discovered.[22–24] Involving the sodium/glucose-cotransporter (sodium-glucose linked transporter; SGLTs), in particular SGLT1,[24] or glucose-transporters (GLUTs) as well as brush border enzymes and ATP-sensitive K^+ channels (K_{ATP}) play a crucial role in this pathway.[20,22,23]

Monitoring the luminal content in various organs to identify potential threats is an integral function of the innate immune system. One type of sentinel cells that take on this task are specialized epithelial cells called tuft-, brush- or chemosensory cells. This cell type expresses the acetylcholine synthesizing enzyme, choline acetyltransferase (ChAT), and utilizes the taste transduction cascade to sense different substances and initiate specific protective mechanisms depending on the organ they are harbored in (reviewed in[25,26]). The transcription factor

Skn-1a/Pou2f3 is required for their development, and its genetic deletion results in their absence in the urethra.[27,28] In the urethra, these sentinel cells used to be called urethral brush cells[29–33] or urethral cholinergic chemosensory cells (UCCC).[34] Recently, the research community decided to designate all these cells with comparable properties and characteristics as tuft cells. Therefore, they are now called urethral tuft cells (UTC). UTC are thought to protect against UTI.[29,33,35] Previously it was shown that tuft cells in the intestine and the trachea express components of the sweet detection pathway, e.g., Tas1R3, but their contribution to sugar sensing in these organs was not investigated so far.[36,37] In the urethra, expression of the *Tas1r3* gene in UTC was described as well.[29] GNAT3 and TRPM5, which are expressed in the urethra exclusively by UTC,[29] are necessary for the detection of sugars by taste cells.[38,39] Whether is detection of sugars by UTC in general remained unclear. We therefore aimed in this study to clarify the mechanism of sugar monitoring in the urethra and which role UTC play in this process.

2. Results

2.1. Expression of Tas1rX in UTC

In previous RT-PCR analyses, we detected only *Tas1r1* and *Tas1r3* in UTC, whereas *Tas1r2* was not detectable.[29] In contrast, next-generation sequencing (NGS) revealed the expression of all three *Tas1rX* family members in at least one of six investigated UTC. *Tas1r2* was expressed in three out of six investigated UTC (**Figure 1A**). We performed RT-PCR with specific primers for *Tas1r1*, *Tas1r2*, and *Tas1r3* of isolated UTC, tongue, and whole urethrae (Figure 1B–D) and enhanced the sensitivity of *Tas1r2* detection by performing nested PCR (Figure 1C). Enhancement of sensitivity of the *Tas1r2* RT-PCR led to a clear detection of all *Tas1rX* family members in isolated UTC and whole urethrae (Figure 1B–D). To validate our data independently we analyzed two independent data sets of single-cell RNA sequencing from urethral tissue provided by the Strand group under the aspects of our study.[40,41] Although these studies only include the prostatic part of the urethra, all cell populations of this section were sequenced. In both data sets, we were able to identify a cell cluster that can be classified as UTC based on the expression of UTC-specific markers. In both datasets, this cluster contains cells expressing UTC markers such as *Trpm5* or *Dclk1*. It also contains *Tas1r3* positive cells (Figures S1 and S2, Supporting Information).

2.2. Calcium Response of UTC Upon Sugar Stimulation

Stimulation with various sugars (25 mM) led to an increase in $[Ca^{2+}]_i$ in UTC isolated from ChAT-eGFP mice (**Figure 2**). The frequency of responding cells differed between sugars. UTC most frequently responded to sucrose (29/37, 78%) (Figure 2A,B). 13 out of 20 (65%) UTC responded to fructose (Figure 2C,D). A response to lactose and maltose was observed in 5 out of 18 (28%) and 6 out of 20 (30%), respectively (Figure 2E–H). Only 3 out of 21 (14%) UTC responded to mannose (Figure 2I,J).

By default, experiments were performed in tyrode III buffer solution containing 10 mM glucose. Using this buffer, already containing glucose 10 mM, only 1 out of 9 (11%) UTC responded to the simulation with glucose 25 mM (**Figure 3A,C**). In experiments with buffer containing no glucose 10/19 (53%) UTC responded to glucose (Figure 3B,C). Comparing both conditions showed a significant difference in the relative frequency of responses ($p = 0.0356$, Figure 3C). This indicates a sensitization of UTC in the presence of glucose or sugars. In another experiment, it was tested if a single UTC respond to various stimuli. Seven of the 29 (24%) investigated UTC responding to sucrose also responded when stimulated with glutamate and denatonium (Figure 3D).

2.3. Sucrose Response of UTC Is Tas1R3 Dependent

For further investigation, we chose 25 mM sucrose stimulation, because 78% of UTC responded initially to sucrose making this the sugar most frequently causing a response of all tested sugars (Figure 2). To determine whether UTC express Tas1R3 on the protein level we utilized Tas1R3-WGA-reporter mice. Immunohistochemistry of urethrae from Tas1R3-WGA mice revealed that all anti-WGA antibody labeled $Tas1R3^+$ cells are also labeled with anti-DCLK1 antibodies. The combination of both antibodies revealed that in urethral epithelium Tas1R3 expression is restricted to UTC (**Figure 4A**).

To clarify the role of UTC and Tas1R3 in urethral sugar sensing we utilized Tas1R3-KO and ChAT-eGFP mice and quantified the calcium response to sucrose of isolated UTC. Moreover, we utilized UTC-deficient (Pou2f3-KO) and Tas1R3-KO mice and quantified the calcium response of isolated urethral cells in the field of view. These experiments showed that the relative frequency of responding UTC was significantly lower in Tas1R3-KO mice (10/26; 38%) compared to the corresponding wildtype (9/10; 90%; $p = 0.025$; Figure 4B). In addition, of those UTC that responded to sucrose, the $[Ca^{2+}]_i$ response was significantly lower in UTC from Tas1R3-KO mice compared to the ones from corresponding wildtypes ($p = 0.0133$; Figure 4C,D). A significantly reduced response was also observed in the presence of the Tas1R3 inhibitor gurmarin ($p = 0.0038$; Figure 4E,F), but neither genetic deletion of Tas1R3 nor gurmarin fully abolished the response.

In Pou2f3-KO mice, 22% (155/716) of the isolated urethral cells responded to sucrose, showing a strong contrast to the corresponding Pou2f3-WT mice, where ≈53% (118/223) of the cells responded ($p > 0.0001$; **Figure 5A**). This finding indicates that UTC are responsible for a considerable proportion (>59%) of sugar perception in the urethra. Comparable results were observed in Tas1R3-KO mice in which 25% (168/632) of the cells responded to sucrose stimulation in contrast to Tas1R3-WT mice where ≈54% (288/519) of the cells responded ($p > 0.0001$; Figure 5B). Thus 54% of responses were Tas1R3 dependent. Application of sucrose to isolated non-tufted cells from ChAT-eGFP mice showed a comparable response as observed in cells from Tas1R3-WT or Pou2f3-WT mice (135/265; Figure S3, Supporting Information). This also indicates that about half (41-46%) of the recognition events are mainly UTC independent since they occurred in both Tas1r3-KO and Pou2f3-KO.

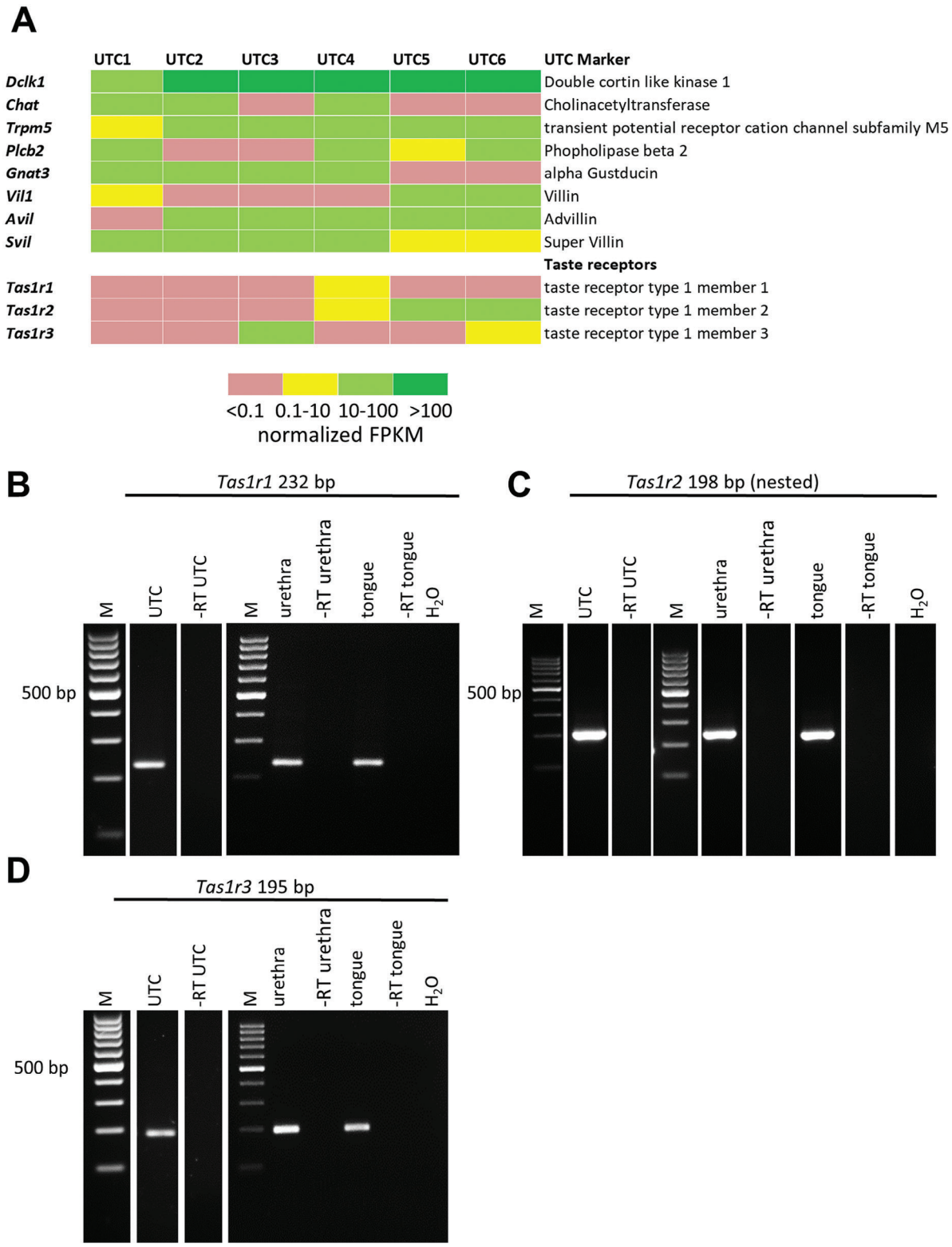

Figure 1. Expression of *Tas1rX* genes in UTC. A), Single UTC determined by NGS Heatmap displaying the detection levels as normalized FPKM in GFP-positive UTC of ChAT-eGFP mice. FPKM = Fragments Per Kilobase Million. Shown is expression of UTC markers and taste receptors *Tas1r1-3*. B–D), RT-PCR of urethral epithelium and isolated UTC. Total RNA was isolated from dissected tissue (urethra or tongue) or pooled isolated cells ($n = 2$ to 6 samples). Isolation of UTC was performed by TRPM5 antibody labeling and separation with magnetic beads. The experiment was repeated 7 times with total number of 35 animals. B), *Tas1r1* (232 bp), C), *Tas1r2* (198 bp) was detected by nested PCR, D), *Tas1r3* (195 bp), +/− RT = aliquots processed with/without reverse transcription; H_2O = water control.

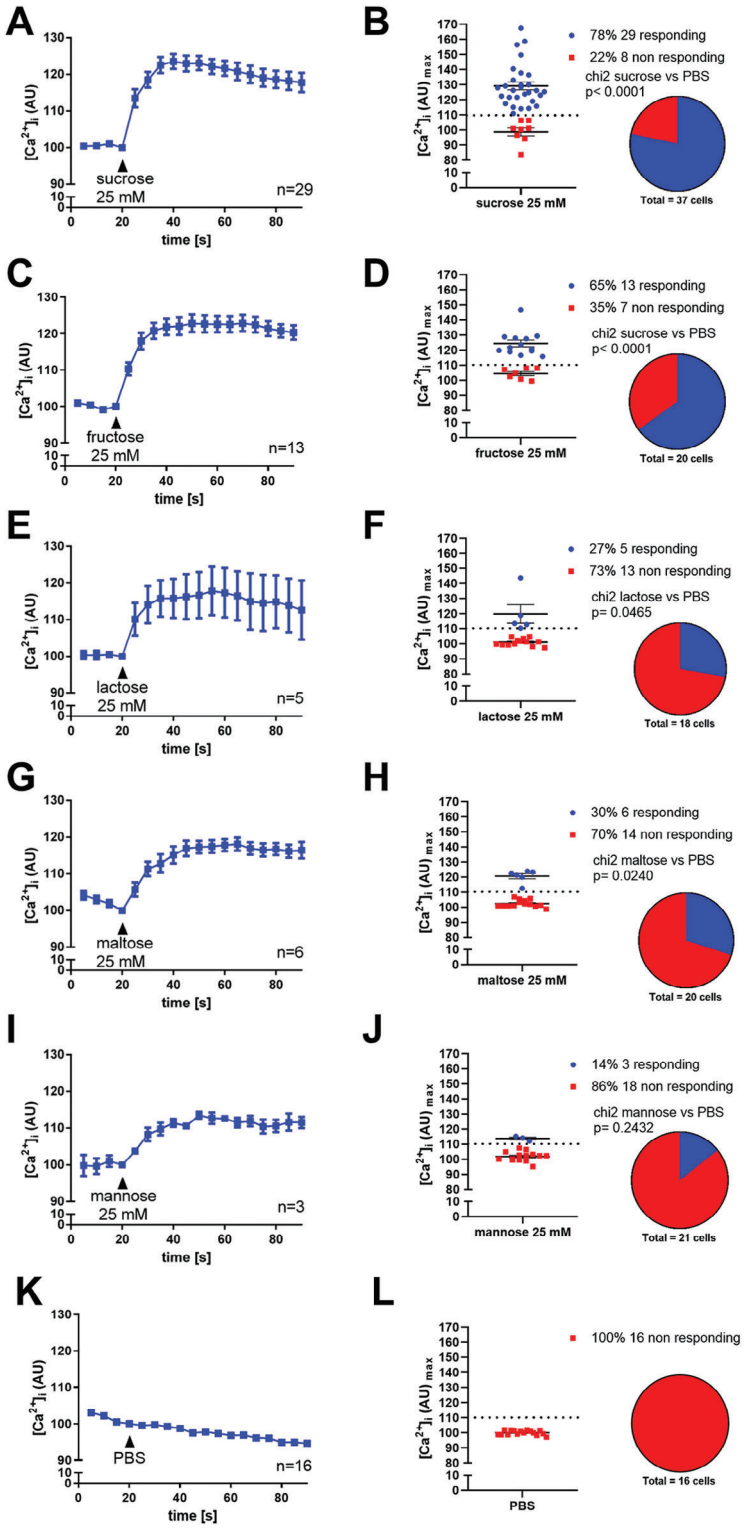

Figure 2. UTC responds to various sugars. Urethral epithelial cells of ChAT-eGFP reporter mice were isolated and UTC were identified by eGFP fluorescence. Y-Axis depicts arbitrary units (AU) of Calcium Orange fluorescence recorded by confocal laser scanning microscopy, correlating to $[Ca^{2+}]_i$. A,C,E,G,I), $[Ca^{2+}]_i$ of responding UTC shown as mean and SEM of intracellular calcium recording. B,D,F,H,J), Maximal calcium response $[Ca^{2+}]_i$ $(AU)_{max}$; Left graph shows changes of $[Ca^{2+}]_i$ in individual cells, dotted line shows increase of $[Ca^{2+}]_i$ by 10% which was used as an indication for responsiveness; Pie charts show percentage representation of tested UTC. A,B), Sucrose, C,D), fructose, E,F), lactose, G,H), maltose, I,J), mannose. K,L), $[Ca^{2+}]_i$ responds UTC to PBS and maximal calcium response $[Ca^{2+}]_i$ $(AU)_{max}$ to PBS together with percentage representation of tested UTC. For statistical analysis of categorical variables chi(2) test was used.

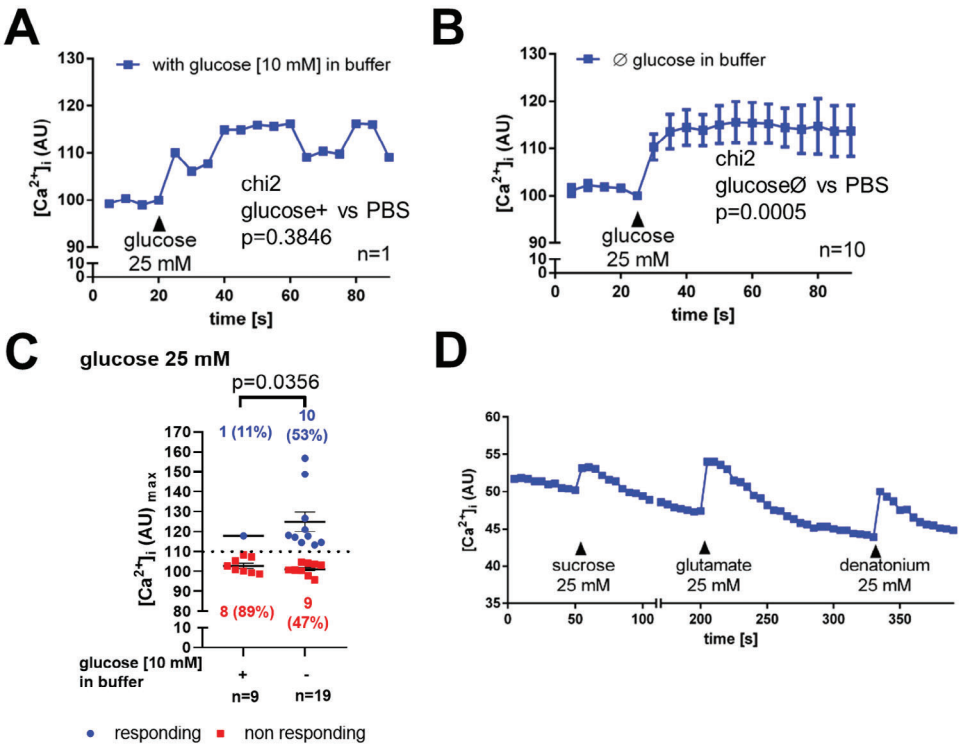

Figure 3. Glucose response of UTC. A), Application of glucose evokes in the presence of 10 mM glucose in the buffer an increase in $[Ca^{2+}]_i$ in only one out of 9 tested cells. Shown is $[Ca^{2+}]_i$ recording of the responding cell. B), In buffer without glucose the number of UTC responding to glucose with an increase in $[Ca^{2+}]_i$ increases to 9 of 19. Shown is $[Ca^{2+}]_i$ recording of responding cells. (A+B), Shown are the mean and SEM of $[Ca^{2+}]_i$ recording. C), Percentage of glucose responding and non-responding UTC with or without glucose in the buffer as well as maximal calcium response $[Ca^{2+}]_i$ $(AU)_{max}$ of individual cells, dotted line shows increase of $[Ca^{2+}]_i$ by 10% which was used as an indication for responsiveness; For statistical analysis of categorical variables chi(2) test was used. D), UTC are polymodal. Representative $[Ca^{2+}]_i$ recording of a single UTC responding to sucrose, glutamate, and denatonium (25 mM each).

2.4. Role of the Tas1R3 Independent Sweet Detection Pathways on Sucrose Detection in the Urethra

An explanation for the previously described findings is a Tas1R3 independent sweet detection pathway. NGS data revealed several components of these pathways in UTC (Figure S4, Supporting Information), but immunohistochemical investigations did not lead to a clear labeling of UTC only. Instead, the whole urethral epithelium was labeled by antibodies against components of this Tas1R3 independent sweet detection pathway (Figures S5 and S6, Supporting Information). RT-PCR experiments of the urethra support the expression of these components in the whole urethral epithelium (Figure S7, Supporting Information) and these components were also detectable by RT-PCR in the urethrae from Pou2f3 mice, harboring no UTC (Figure S8, Supporting Information). Analyses of the two independent data sets of single-cell RNA sequencing from urethral tissue provided by the Strand group[40,41] revealed that components of the Tas1R3 independent sweet detection pathway, like *Sc5α1* (SGLT1) and *Abcc8* (sulfonylurea receptor 1; SUR1), are rather ubiquitously expressed (Figures S1 and S2, Supporting Information). This goes side by side with our findings that a calcium response to sugar stimulation is still measurable in Pou2f3-KO mice (Figure 5A) and strengthens the assumption that the Tas1R3 independent sweet detection pathway is present in various cells of the urethral epithelium and not limited to UTC.

To investigate whether this pathway may be responsible for the response in the absence of Tas1R3 and in Pou2f3-KO mice, we quantified the calcium response of isolated cells from Pou2f3-KO and WT mice to glibenclamide. Glibenclamide, a K^+-ATP channel antagonist, binds and inhibits the ATP-sensitive potassium channels (K_{ATP}) inhibitory regulatory subunit SUR1. This inhibition causes cell membrane depolarization and opening of voltage-dependent calcium channels (Figure S4A, Supporting Information). This is the same mechanism that is used for the Tas1R3 independent recognition of sugars. Therefore, it is used to activate the Tas1R3 independent sweet detection pathway.[22]

Interestingly, 22% (46/203) of the cells from Pou2f3-KO mice and 18% (43/241) of the cells from Pou2f3-WT mice responded to glibenclamide, and therefore via the Tas1R3 independent sweet detection pathway (Figure 5C). A comparable result could be observed in Tas1R3-KO and Tas1R3-WT mice, 14% (17/122) and 11% (40/373), respectively, of the cells that responded to glibenclamide (Figure 5D). These findings strengthened our previous results showing that about half of recognition events are mainly UTC independent and operate through the Tas1R3 independent sweet detection pathway. Finally, we conducted the sucrose stimulation experiment in Tas1R3-KO and Tas1R3-WT mice in the

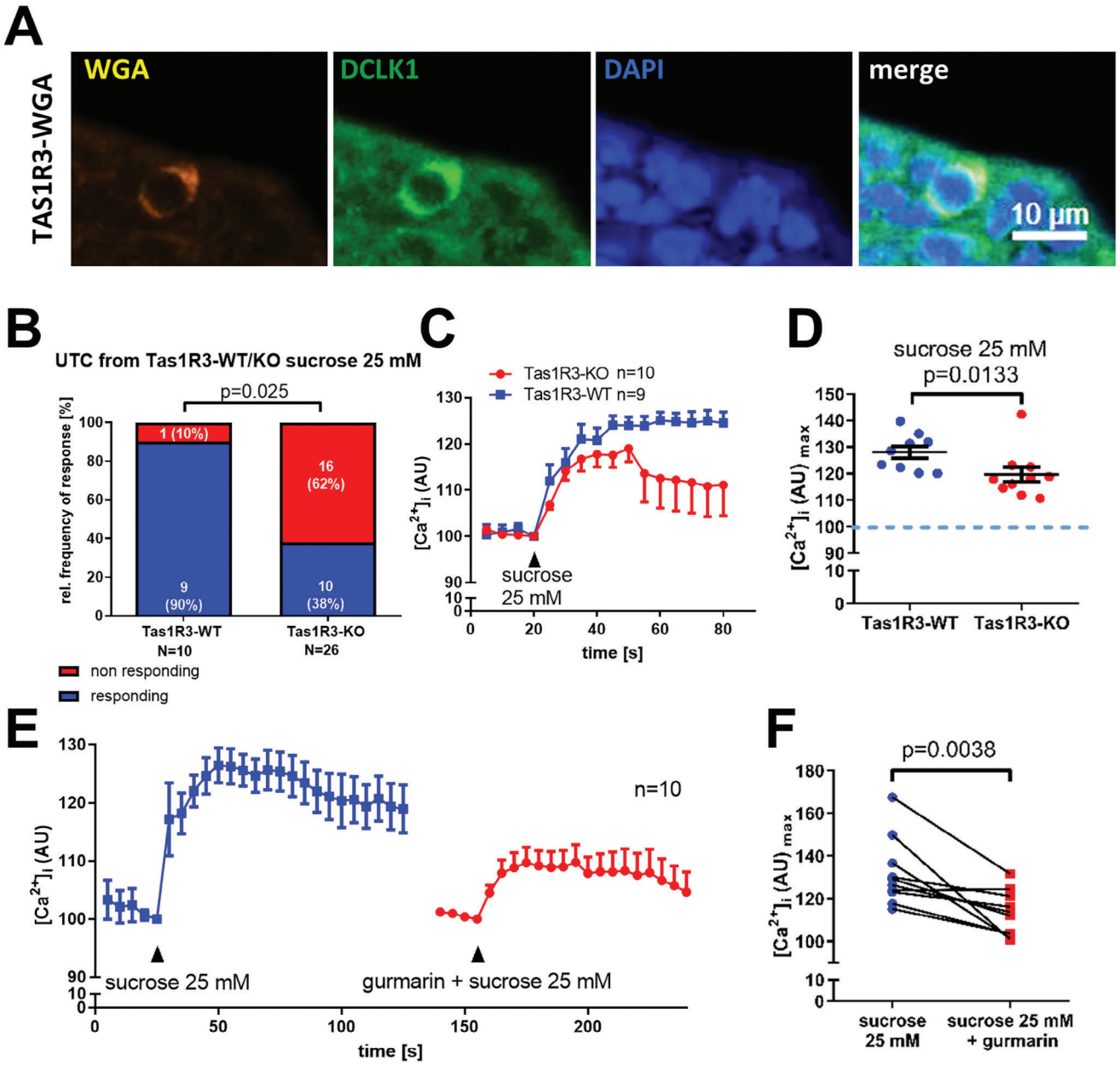

Figure 4. UTC response to sucrose is Tas1R3 dependent. A), Double-labeling of UTC in Tas1R3-WGA reporter mice. Tas1R3 expression is shown utilizing WGA-immunoreactivity visualized with Cy3-conjugated secondary antisera. UTC identification is performed by UTC marker DCLK1-immunoreactivity visualized with FITC-conjugated secondary antisera. WGA, DCLK1, DAPI, and merge are shown. Scale bar represents 10 µm throughout. B), Percentage representation of sucrose responding UTC from Tas1R3-KO mice and corresponding WT. Increase of $[Ca^{2+}]_i$ by 10% was used as indication for responsiveness. For statistical analysis of categorical variables chi(2) tests were used. (C+D), Urethral epithelial cells of Tas1R3-KO mice and corresponding WT were isolated and UTC were identified by TRPM5 antibody labeling. C), Y-Axis depicts arbitrary units (AU) of Calcium Orange fluorescence recorded by confocal laser scanning microscopy, correlating to $[Ca^{2+}]_i$, shown are mean and SEM. D), Statistical analysis of maximal calcium response $[Ca^{2+}]_i$ $(AU)_{max}$ of UTC from Tas1R3-KO mice and corresponding WT mice response to sucrose shown in C) with Mann–Whitney test. (E+F), Urethral epithelial cells of ChAT-eGFP reporter mice were isolated and UTC was identified by eGFP fluorescence. Response to sucrose and to sucrose in the presence of gurmarin (Tas1R3 inhibitor) was measured E), shown are mean and SEM. Y-Axis depicts arbitrary units (AU) of Calcium Orange fluorescence recorded by confocal laser scanning microscopy, correlating to $[Ca^{2+}]_i$. F), Statistical analysis of maximal calcium response $[Ca^{2+}]_i$ $(AU)_{max}$ of UTC response shown in E) to sucrose compared to sucrose in the presence of gurmarin (1 µg mL^{-1}). For statistical analysis, paired *t*-test was used.

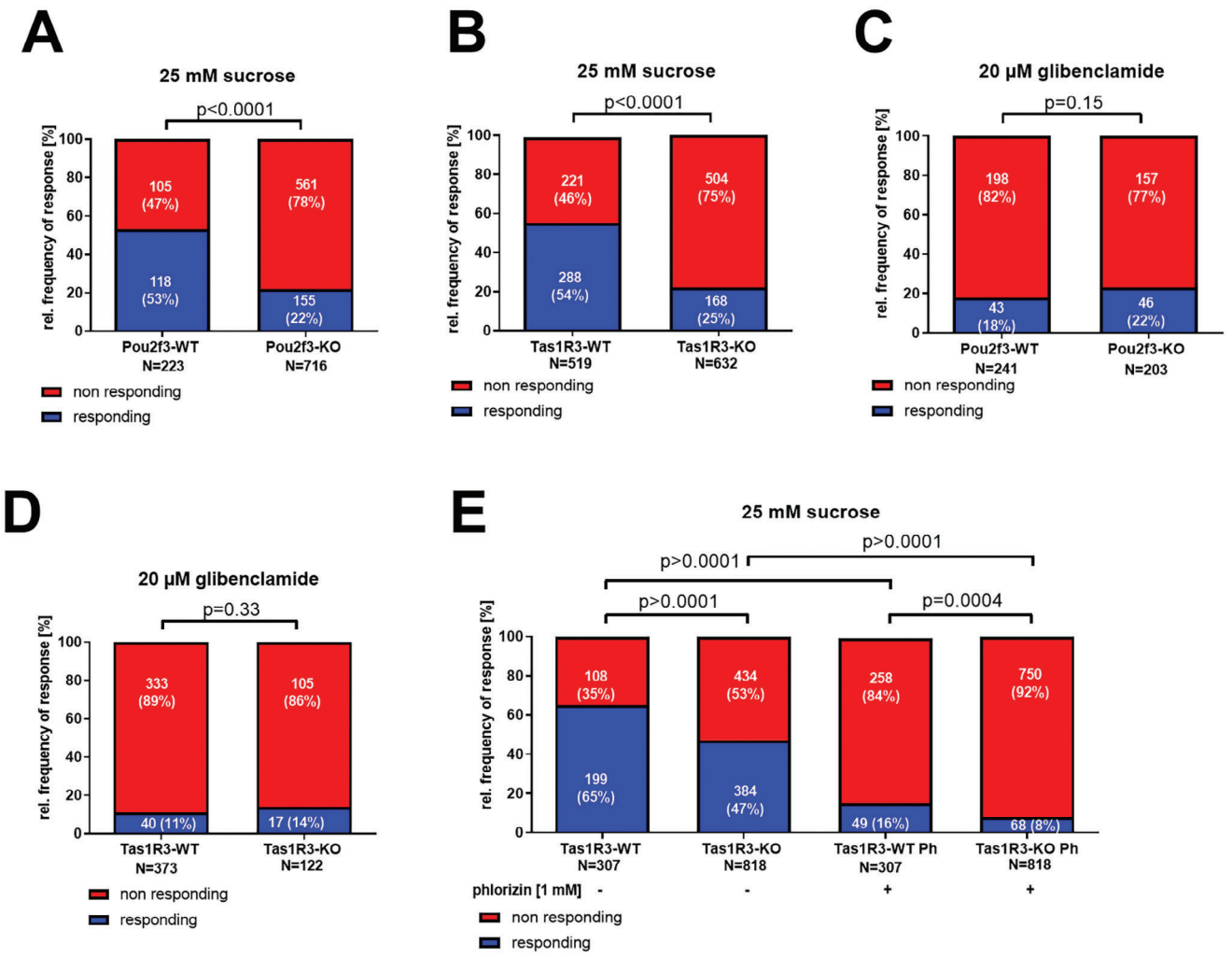

Figure 5. Impact of the Tas1R3 independent sweet detection pathway on sweet detection in the urethra. Urethral cells of Pou2f3-KO and Tas1R3-KO mice and corresponding WT mice were isolated. Arbitrary units (AU) of Calcium Orange fluorescence recorded by confocal laser scanning microscopy, correlating to $[Ca^{2+}]_i$ response of isolated cell in the field of view was quantified. Increase of $[Ca^{2+}]_i$ by 10% was used as indication for responsiveness. A), Cells from Pou2f3-WT/KO in presence of 25 mM sucrose B), Cells from Tas1R3-WT/KO in presence of 25 mM sucrose C), Cells from Pou2f3-WT/KO in presence of 20 µM glibenclamide D), Cells from Tas1R3-WT/KO in presence of 20 µM glibenclamide. E), Cells from Tas1R3-WT/KO in presence of 25 mM sucrose with or without 1 mM phloridizin. For statistical analysis of categorical variables chi(2) tests were used.

presence or absence of phlorizin, an SGLT1 inhibitor and, therefore, an inhibitor of the Tas1R3 independent sweet detection pathway (Figure S4A, Supporting Information). Confirming our previous results, we observed a significant difference between Tas1R3-KO (47%; 384/818) and Tas1R3-WT mice (65%; 199/307; $p > 0.0001$) in the number of cells responding to sucrose without the addition of phlorizin. In the presence of phlorizin, only 16% (49/307) of the cells from Tas1R3-WT mice responded to sucrose. Moreover, phlorizin is acting additive to the genetic knockout of Tas1R3. In the presence of phlorizin, a significantly lower number of cells compared to Tas1R3-WT mice (8%, 68/818, $p = 0.0004$; Figure 5E) responded to sucrose. This finding indicates that sugar monitoring in the urethra occurs via two distinct pathways: A Tas1R3-dependent pathway that is exclusive to UTC, and a Tas1R3-independent way not exclusive to UTC.

2.5. Intraurethral Sugar Application Increases Detrusor Activity

In the following, we performed urodynamic investigations to determine whether the perception of sugars in the urethra has physiological relevance. Urodynamic investigations in combination with intraurethral stimulation are hardly possible in mice due to their small size and high susceptibility to anesthetic incidents. Therefore, we utilized urethane-anesthetized rats. Rats as well as other mammals are known to harbor UTC in the urethral epithelium.[27,28] We inserted a catheter into the bladder dome and filled the bladder continuously with saline solution (0.04 mL min^{-1}). Fast filling of the bladder caused cycles of rising intravesical pressure and micturition. Urethral instillation of saline solution (NaCl 0.9%; 50 µL) through the external urethral orifice augmented pressure rises only slightly, but a single dose

of sucrose (25 mM; 50 µL) significantly increased detrusor activity compared to NaCl application ($p = 0.023$), causing washout or at least a drastic dilution of urethral content (**Figure 6**A,B). In contrast, a combined application of sucrose and the Tas1R3 inhibitor gurmarin did not lead to increased detrusor activity ($p = 0.67$; Figure 6C–E), comparable to the NaCl application. We repeated the experiment with glucose. Application of glucose led to a comparable result. A single dose of glucose (25 mM; 50 µL) significantly increased detrusor activity compared to NaCl application ($p = 0.0433$; Figure 6F,H). In contrast, a combined application of glucose and the Tas1R3 inhibitor gurmarin did not lead to an increased detrusor activity ($p = 0.2451$; Figure 6G,I,J), compared to the NaCl response. These results indicate that intraurethral sweet stimulation increases the activity of the Musculus detrusor vesicae. This response seems to be Tas1R3 and therewith UTC dependent.

3. Discussion

This study aimed to clarify the mechanism of sugar monitoring in the urethra and which role UTC plays in this process. Our experiments showed that sugar monitoring in the urethra occurs via two distinct pathways. On the one hand, a Tas1R3-dependent signaling pathway that occurs exclusively in UTC and is involved in the initiation of defense mechanisms. On the other hand, a Tas1R3-independent signaling pathway is found in both UTC and other urethral epithelial cells.

Interestingly, the NGS of UTC did not show ubiquitous *Tas1r1*, *Tas1r2*, or *Tas1r3* expression in the cells. Accordingly, not all UTC respond to sugars. Even in the group with the highest responsiveness, ≈22% of UTC did not respond to stimulation. Moreover, even in UTC taken from ChAT-eGFP mice and selected by ChAT promoter-regulated eGFP expression, *Chat* expression was not ubiquitous in all 6 UTC. This highlights the fact that the actual mRNA level represents only a snapshot and does not necessarily correspond 1:1 to the actual protein level.

The fact that neither investigations in Tas1R3-KO mice nor the application of Tas1R3 inhibitor gurmarin resulted in complete inhibition in any test system we used suggests that an alternative detection mechanism must be present. The observed activation of the Tas1R3 independent sweet detection pathway with glibencamide resulted in a comparable number of responding cells, pointing towards a Tas1R3 independent sweet detection pathway as well and display an additional recognition mechanism. This assumption is supported by the observation that blocking this pathway and knocking out Tas1R3 together almost fully abrogated the response to sucrose in isolated urethral cells. The observation that the amount of responding cells does not correlate with the amount of UTC lacking in the KO animals can be explained by the distinct way tuft cells work. It is known from experiments in the respiratory tract[42] and in the urethra[29,31] that tuft cells activate neighboring cells after they have been activated by the release of second messenger substances such as acetylcholine. As a result, the number of reacting cells is higher than the number of tuft cells.

The clinical relevance of these findings is still unclear. However, increased sugar concentrations in the urine promote the growth of pathogenic bacteria.[10–14] Accordingly, an increased sugar concentration displays a potential threat that should be recognized and addressed. A task that our data suggest is performed by UTC.

Under physiological conditions, sugar plays a subordinate role in the composition of urine. Normally, there is little to no glucose within the urine.[43,44] Nevertheless, small quantities of intact dietary sucrose, lactose, and fructose are subsequently excreted in the urine.[45] Urinary sucrose has been used in several studies as a biomarker of sugar consumption and total sugar intake.[46–52] This is possible because small amounts of sucrose evade hydrolysis by sucrase and can be absorbed in the jejunum as a disaccharide instead of being cleaved into glucose and fructose.[45,52] Circulating sucrose, unlike glucose, is excreted in the urine.[53] At most, ≈0.05% of consumed sucrose is excreted in the urine and detected in samples after 24 h of consumption, but this small amount correlates very well with sugar intake under controlled dietary intake and urination conditions ($r = 0.88$).[52] But excretion of sucrose and lactose into urine increases enormously up to a level of 33 mM in patients suffering from gastroenteritis, coeliac disease, hiatus hernia, sucrosuria, and other intestinal abnormalities.[45,54–58] This has been attributed to either disaccharidase deficiency producing elevated intestinal concentrations, or increased permeability of a structurally damaged mucosa.[45,54–57]

An increase in the urine sugar concentration is ubiquitous in diabetic diseases.[10–14] In buffer solution already containing glucose, UTC showed a diminished response to an increase of glucose concentration. These findings indicate that UTC can be desensitized and thereby decreasing their protective abilities. High glucose concentration in DM patients, comparable with a higher glucose level in the buffer may lead to such a desensitization of UTC. Consequently, the protective mechanisms triggered by UTC would not work properly and the risk of infection would increase in these patients. Interestingly, an increased risk for UTI infection is a common comorbidity of diabetes.[1–7] In addition, ≈50% of DM patients suffer from bladder dysfunction, cystopathy, and an overactive bladder,[59] diseases connected to mechanisms that might be influenced by UTC.[29,33,35] In a clinical drug trial in Japan a group of thirteen type 2 DM patients showed mean pre-treatment urine glucose levels of 39 mmol l^{-1}.[60] Frequently used commercially available dipstick tests detect urine glucose levels as high as 111 mmol l^{-1} (Combur 10 urine test strips, Roche, Basel, Switzerland). This confirms that the concentration we used in our experiments is within the range of sugar concentrations reached in pathophysiological conditions in humans and therefore of clinical relevance.

The importance of Tas1R3 signaling in chemosensory cells is not limited to the urethra. Recently Howitt and colleagues reported that Tas1R3 in tuft cells of the intestinal tract regulates the homeostasis of these cells.[37] Lee and colleagues showed that the presence of sugars especially of glucose diminish in a Tas1R3 mediated way the defensive response of sinonasal solitary chemosensory cells to the bitter compound denatonium. In contrast to UTC, the application of sugars alone shows no effects on de novo calcium signaling in these cells.[61]

So far it is known that UTC recognizes bitter substances,[29] high levels of salt,[32] free amino acids ("umami"), and heat-inactivated uropathogenic *Escherichia coli* (UPEC).[29] We expand the group of substances stimulating UTC by various sugars thereby expanding the group of taste qualities recognized by UTC. In previous studies we showed that UTC responds to bitter,

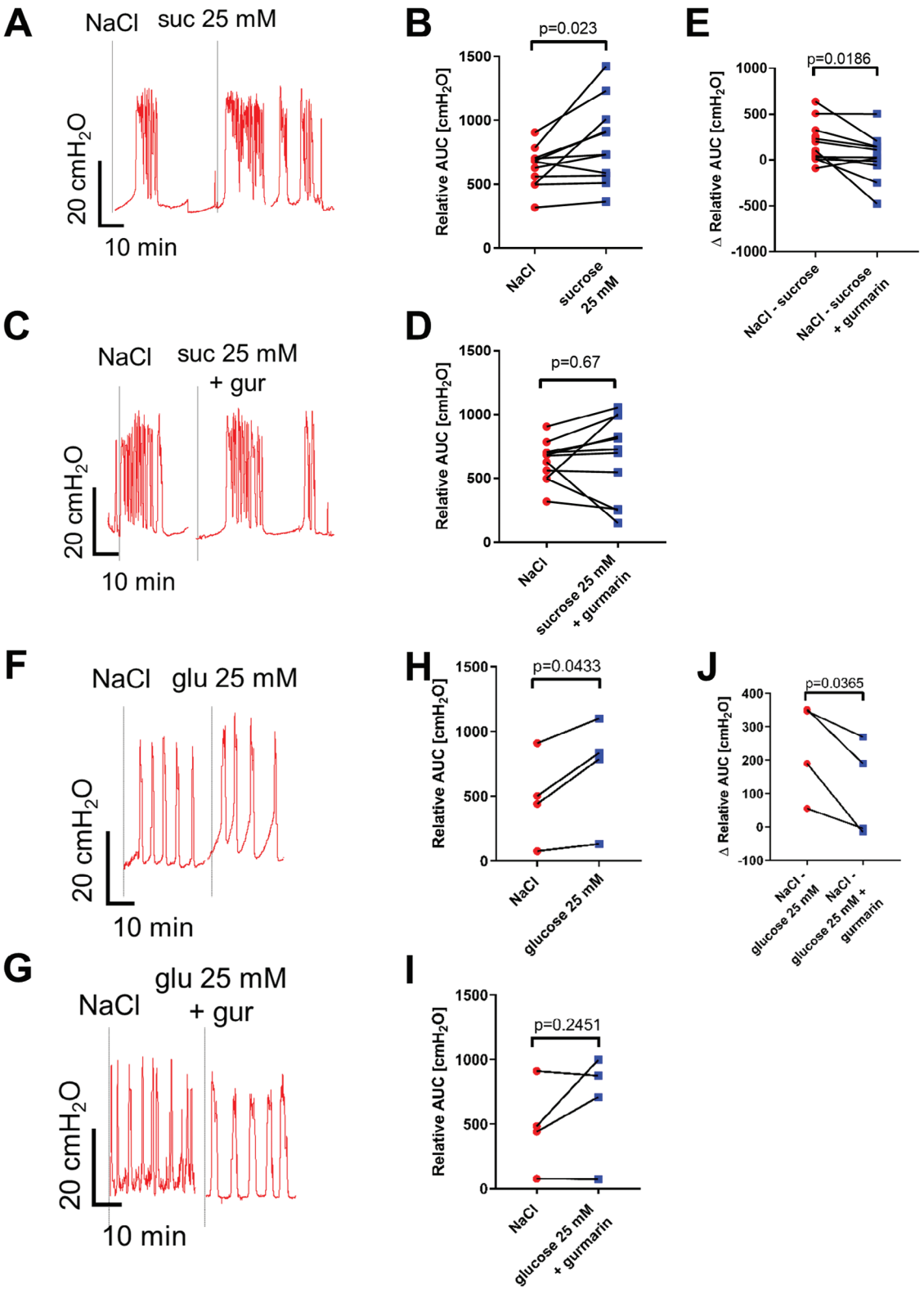

Figure 6. Intraurethral sugar application increases detrusor muscle activation in a Tas1R3 dependent manner. Cystometric recordings from urethane-anesthesized rats. The bladder was continuously filled with saline (0.04 mL min^{-1}), causing a rise in intravesical pressure and initiating detrusor contraction and micturition. (A+F), Original recording of urethral instillation of A) sucrose (25 mM) and F) glucose (25 mM) increases detrusor activity compared with saline (NaCl) application alone. (B+H), Detrusor activity after instillation of sucrose B) and glucose (H) compared with saline (NaCl) application quantified as area under the curve (AUC). (C+G), Original recording of urethral instillation of a combination of C) sucrose (25 mM) or (G)

umami, and salty in a polymodal manner, proving their ability to react on several different stimuli. This study supports the polymodal character of UTC we observed in previous studies.[29,32]

4. Conclusion

Sugar monitoring in the urethra occurs via two distinct pathways. A Tas1R3-dependent pathway that is exclusive to UTC, that is also involved in the initiation of defense mechanisms, and a Tas1R3-independent way, which can be found both in UTC and in other epithelial cells of the urethra. In addition, we could show that UTC responds to various sugars.

5. Experimental Section

Animals: C57BL6/J mice, ChAT-eGFP mice (B6.Cg-Tg(RP23-268L19-EGFP)2Mik/J; Stock No. 007902), Tas1R3-KO mice (B6;129-Tas1r3tm1Csz/J; Stock No. 013066) and corresponding wildtypes (Tas1R3-WT, litter mates of Tas1R3-KO mice), and Wistar Rats were obtained from Jackson Laboratory (Bar Habor, ME, USA). Pou2f3-KO mice (B6.129-Pou2f3tm1Abek) and Tas1R3-WGA mice (Tg(T1r3-WGA)tm1Abek)[62] were provided by R. Margolskee and I. Matsumoto, respectively. Animals were housed in the animal facility of the Justus-Liebig-University Giessen under specific pathogen free (SPF) conditions (10 h dark, 14 h light), with free access to food and water. This study was carried out in accordance with the recommendations of the European Communities Council Directive of 24th November 1986 (86/609/EEC). The protocol was approved by the Committee for Animal Welfare (Regierungspräsidium Giessen, Germany; reference no. 572_M, 632_M, 641_M and V54-19 c 20 15 h 01 GI20/25 Nr. G22/2017).

Cell Isolation: Cell isolation was performed as described previously.[29] In brief: Urethrae were dissected, cut into small pieces, and enzymatically digested in dispase (2 mg mL^{-1}; Sigma–Aldrich/Merck, Darmstadt, Germany) and trypsin/PBS (1:1, Invitrogen, Carlsbad, CA, USA). After mechanical dissociation, the cell suspension was passed through a cell strainer (pore size 70 µm; BD Bioscience, Franklin Lakes, NJ, USA). UTC was identified by eGFP fluorescence or by immunolabelling with a rabbit polyclonal TRPM5-antibody (OST00106W, Osenses Pty Ltd, Keswick, Australia) directed against an extracellular domain and magnetic beads (Invitrogen) coated with goat anti-rabbit IgG (H+L) (PI65-6100; Invitrogen), followed by harvesting through immunomagnetic cell separation.

Next Generation Sequencing: NGS was performed as described elsewhere.[63] In brief: Isolated single eGFP-positive cells were identified, picked, and transferred to a PCR tube using a combined confocal laser-scanning/patch-clamp setup (Leica TCS SP5, Leica Microsystems/Luigs-Neumann, Wetzlar/Ratingen, Germany). Cell lysis, cDNA synthesis, and amplification were performed using the Sigma SeqPlex RNA Amplification Kit (Sigma–Aldrich/Merck, Darmstadt, Germany). For library preparation, the Illumina Nextera XT DNA sample preparation protocol (Part # 15031942 Rev. C) was used. Samples were run together with a 2 × 75 bp read length using the MiSeq Reagent Kit v3 (150 cycles) and the Illumina MiSeq Desktop Sequencer (Illumina, San Diego, CA, USA). The sequencing reads were aligned to the mm9 reference genome and transcriptome using TopHat2 (2.0.9). The TopHat output files were saved in BAM format and evaluated by Cuffdiff2 (2.1.1). All samples were compared and evaluated in one calculation cycle, allowing the algorithm to estimate the Fragments Per Kilobase Million (FPKM) values at the transcript level resolution and to control for variability across the replicate libraries.

Analyses of Single-Cell RNA Sequencing from Urethral Tissue: Two independent data sets of single-cell RNA sequencing were analyzed from urethral tissue provided by the Strand group under the aspects of this study. These data are publicly available and can be found at http://strandlab.net/sc.data/.[40,41]

RT-PCR: Total RNA was isolated from dissected urethra or pooled isolated cells ($n = 2$ to 6 samples). Isolation of UTC was performed by TRPM5 antibody labeling and separation with magnetic beads. The experiment was repeated seven times with the total number of 35 animals. For RNA extraction the Qiagen RNeasy Micro Kit (Qiagen, Hilden, Germany) was used according to the manufacturer's protocol. Extracted total RNA from tongue was used as positive control. RT-PCR was performed as described previously.[29] Primer sequences are listed in Table S1 (Supporting Information). For detection of Tas1r2 nested PCR with equal condition was performed.

Immunofluorescence: Urethrae of Tas1R3-WGA (wheat germ agglutinin) mice ($n = 3$) used for immunofluorescence were provided by I. Matsumoto. Tissue was fixed by transcardiac perfusion with phosphate-buffered 4% paraformaldehyde. Specimens were washed in 0.1 M phosphate buffer and embedded in paraffin (Paraplast Plus, Leica, Nussloch, Germany) or incubated overnight in 18% sucrose (Carl Roth, Karlsruhe, Germany) in 0.1 M phosphate buffer, embedded in Tissue-Tek O.C.T. Compound (Sakura Finetek Germany GmbH, Staufen, Germany) and frozen in liquid nitrogen. Primary antibody was applied to 4–18 tissue sections (frozen 10 µm or paraffin 5 µm). Unspecific protein binding sites were saturated by incubation with 10% horse serum (PAA Laboratories Inc., Pasching, Austria), 1% bovine serum albumin (Sigma–Aldrich/Merck, Darmstadt, Germany), 0.5% Tween (Sigma–Aldrich/Merck, Darmstadt, Germany) in 0.005 M phosphate buffer for 2 h. Primary antibodies were diluted in 0.005 M phosphate buffer and applied overnight at 4 °C. Then, sections were rinsed repeatedly, covered with appropriate fluorophore-conjugated secondary antibodies for 1 h at room temperature, rinsed, post-fixed with phosphate-buffered 4% paraformaldehyde, and mounted in carbonate-buffered glycerol (pH 8.6) containing 1 µg mL^{-1} 4′,5-diamidino-2-phenylindole (DAPI; Sigma–Aldrich). Primary antibodies were rabbit-anti WGA (ab178444; 1:200 dilution; Abcam, Cambridge, UK), sheep-anti-DCAMKL1 (fserine/threonine-protein kinase DCLK1 (doublecortin-like kinase 1); af7138, 1:400 dilution; R&D System, Minneapolis, MN, USA), rabbit-anti Glut2 (H-67; 1:50 dilution; Santa Cruz Biotechnology, Dallas, TX, USA), rabbit-anti Glut4 (ab33780; 1:250 dilution; Abcam, Cambridge, UK), rabbit-anti Kir6.1/KCNJ8 (Q2524576; 1:50 dilution; Millipore/Merck, Darmstadt, Germany), rabbit-anti Kir6.2 (ab79171; 1:50 dilution; Abcam, Cambridge, UK) and rabbit-anti SUR-1 (H-80; 1:50 dilution; Santa Cruz Biotechnology, Dallas, TX, USA), Secondary antibodies were donkey-goat IgG (H+L) conjugated to Alexa Fluor 488 (A11055; 1:1000; Merck, Darmstadt, Germany) and donkey-anti-rabbit IgG Cy3 (2567112; 1:2000; Merck, Darmstadt, Germany). Specificity of secondary reagents was validated by the omission of primary antibodies. Sections were evaluated by epifluorescence microscopy (Axioplan 2, Zeiss, Jena, Germany) or confocal laser scanning microscope (LSM 710, Zeiss, Oberkochen, Germany). Overlay images were created using ImageJ. Each incubation setup was performed at least three times.

Measurement of Intracellular Calcium Concentration: Measurement of intracellular calcium concentration ($[Ca^{2+}]_i$) was performed as described previously.[29] In brief: Isolated cells were loaded with the fluorescent calcium indicator Calcium Orange AM (0.01 µg $µL^{-1}$; Thermo Fisher Scientific Inc., Waltham, MA, USA) and plated on coverslips. $[Ca^{2+}]_i$ was

glucose (25 mM) and gurmarin (1 µg mL^{-1}) compared with saline (NaCl) application. (D+I), Detrusor activity after instillation of a combination of D) sucrose (25 mM) or (I) glucose (25 mM) and gurmarin (1 µg mL^{-1}) compared with saline (NaCl) application quantified as AUC. (E+J), Delta of (B or H) compared with delta of (D or I) AUC was determined over a period of 20 min in each condition, in 11 resp. 4 experiments. First recordings were made after NaCl application. Second recordings were made after the application of a single dose of sucrose (25 mM) or glucose (25 mM), third recordings were made after application of a combination of sucrose (25 mM) or glucose (25 mM) and gurmarin (1 µg mL^{-1}). Order of application was changed between experiments. For statistical analysis paired t-tests were used.

analyzed with a confocal laser scanning microscope (LSM 710, Zeiss, Oberkochen, Germany) during continuous perfusion with Tyrode III buffer with or without 10 mM glucose (2.5 mL min^{-1}; 37 °C). Fluorescence intensities at the start of the recording period were set arbitrarily at 100%. Test stimuli were the sugars sucrose, fructose, lactose, maltose, or mannose (all 25 mM; Sigma–Aldrich/Merck, Darmstadt, Germany, diluted in Tyrode III buffer). All test stimuli were tested on isolated cells from at least three different animals. In the previous studies mannitol at the concentration 25 mM as osmolality control was used.[32] Here the same concentration of sugar for stimulation were used. Hence, it is assumed that the observed effects are not due to an osmolarity effect. Tas1R3 inhibitor gurmarin (1 µg mL^{-1}),[64,65] K+ATP channel antagonist glibenclamide (20 µM; G0639; Sigma–Aldrich/Merck, Darmstadt, Germany)[20] and competitive SGLT1 inhibitor phlorizin (1 mM; 272313; Sigma–Aldrich/Merck, Darmstadt, Germany)[24] were dissolved in buffer. For quantification $[Ca^{2+}]_i$ increase of >10% compared to baseline fluorescence intensity was classified as response.

Urodynamic Measurement: Urodynamic measurements were performed as described previously.[29] In brief: Male Wistar Rats were anesthetized by subcutaneous injection of urethane (1.2 g kg^{-1}, Sigma–Aldrich/Merck, Darmstadt, Germany). A catheter (PE50; BD Intramedic, Becton Dickinson, Franklin Lakes, NJ, USA) was surgically inserted into the bladder dome and connected to a pressure transducer and an infusion pump. Saline solution at room temperature was infused into the bladder at a rate of 0.04 mL min^{-1}. After a stabilization phase of 15–30 min, the intravesical bladder pressure was recorded continuously, and 50 µL of test stimuli were administered into the urethral external orifice via a 0.9 × 25 mm cannula (Braun Vasofix G22) mounted on a 100 µL pipette. For final data analysis, areas under the curve (AUC) of equal time periods before and after stimulation were compared; data are presented as AUC/min. The urodynamic recording sessions took 3–4 h for each animal.

Statistical Analysis: Data were analyzed for normal distribution by the Kolmogorov–Smirnov test. For comparison of paired samples paired *t*-test was used. Categorical variables were analyzed by chi-squared test. Statistical analysis was performed with Mann–Whitney test. *P*-values ≤ 0.05 were regarded as statistically significant. Analyses were performed by GraphPad Prism 7 (GraphPad Software Inc., La Jolla, CA, USA).

Supporting Information

Supporting Information is available from the Wiley Online Library or from the author.

Acknowledgements

The author thank W. Kummer for support. The authors thank T. Eiffert and T. Papadakis for skillful technical assistance. This study was awarded the Eugen-Rehfisch-Preis at the Forum Urodynamicum 2019. This work was funded by University Hospital of Giessen and Marburg (UKGM)-Justus-Liebig-University (JLU)-Cooperation Grant #7/2016 GI (KD) Else Kröner–Fresenius–Stiftung grant 2016_A90 (KD).

Open access funding enabled and organized by Projekt DEAL.

Conflict of Interest

The authors declare no conflict of interest.

Author Contributions

P.S. and A.P. contributed equally to this work. Conceptualization and supervision was done by K.D. Methodology was done by S.P., A.P., L.B., and K.D. Investigation and writing—reviewing and editing of the manuscript was done by S.P., M.B., S.W., and K.D. Visualization was done by S.P., A.P., S.W., and K.D. Writing—original draft was done by S.P., A.P., and K.D.

Data Availability Statement

The data that support the findings of this study are available from the corresponding author upon reasonable request.

Keywords

brush cells, chemosensory, cholinergic, gurmarin, sweet, Tas1R3, urinary tract infection

Received: February 28, 2024
Published online: March 28, 2024

[1] J. E. Patterson, V. T. Andriole, *Infect. Dis. Dent. Clin. North Am.* **1997**, *11*, 735.
[2] J. E. Patterson, V. T. Andriole, *Infect. Dis. Dent. Clin. North Am.* **1995**, *9*, 25.
[3] G. G. Zhanel, L. E. Nicolle, G. K. Harding, *Clin. Infect. Dis.* **1995**, *21*, 316.
[4] M. A. J. Beerepoot, C. D. J. den Heijer, J. Penders, J. M. Prins, E. E. Stobberingh, S. E. Geerlings, *Clin. Microbiol. Infect.* **2012**, *18*, E84.
[5] S. E. Geerlings, R. P. Stolk, M. J. Camps, P. M. Netten, J. B. Hoekstra, K. P. Bouter, B. Bravenboer, J. T. Collet, A. R. Jansz, A. I. Hoepelman, *Diabetes Care* **2000**, *23*, 744.
[6] S. E. Geerlings, R. P. Stolk, M. J. L. Camps, P. M. Netten, J. B. L. Hoekstra, P. K. Bouter, B. Braveboer, T. J. Collet, A. R. Jansz, A. M. Hoepelman, *Adv. Exp. Med. Biol.* **2000**, *485*, 309.
[7] C. Schneeberger, B. M. Kazemier, S. E. Geerlings, *Curr. Opin. Infect. Dis.* **2014**, *27*, 108.
[8] S M. Lenherr, J. Q Clemens, B H. Braffett, P A. Cleary, R L. Dunn, J M. Hotaling, A M. Jacobson, C. Kim, W. Herman, J S. Brown, H. Wessells, A V. Sarma, *J Urol* **2016**, *196*, 1129.
[9] O. Nitzan, M. Elias, B. Chazan, W. Saliba, *Diabetes, Metab. Syndr. Obes.* **2015**, *8*, 129.
[10] M.-C. Wang, C.-C. Tseng, An-B Wu, W.-H. Lin, C.-H. Teng, J.-J. Yan, J.-J. Wu, *J. Microbiol. Immunol. Infect.* **2013**, *46*, 24.
[11] R. Fünfstück, L E. Nicolle, M. Hanefeld, K G. Naber, *Clin. Nephrol.* **2012**, *77*, 40.
[12] S. L. Chen, S. L. Jackson, E. J. Boyko, *J. Urol.* **2009**, *182*, S51.
[13] F. Daneshgari, G. Liu, L. Birder, A. T. Hanna-Mitchell, S. Chacko, *J. Urol.* **2009**, *182*, S18.
[14] S E. Geerlings, R. Meiland, E C. van Lith, E C. Brouwer, W. Gaastra, A I. M. Hoepelman, *Diabetes Care* **2002**, *25*, 1405.
[15] A A. Pezzulo, J. Gutiérrez, K S. Duschner, K S. McConnell, P J. Taft, S E. Ernst, T L. Yahr, K. Rahmouni, J. Klesney-Tait, D A. Stoltz, J. Zabner, *PLoS One* **2011**, *6*, e16166.
[16] J. P. Garnett, E. H. Baker, D. L. Baines, *Eur. Respir. J.* **2012**, *40*, 1269.
[17] A. A. Bachmanov, G. K. Beauchamp, *Annu. Rev. Nutr.* **2007**, *27*, 389.
[18] G Q. Zhao, Y. Zhang, M A. Hoon, J. Chandrashekar, I. Erlenbach, N J. P. Ryba, C S. Zuker, *Cell* **2003**, *115*, 255.
[19] N. Chaudhari, S. D. Roper, *J. Cell Biol.* **2010**, *190*, 285.
[20] S. K. Sukumaran, S. R. Palayyan, *Int. J. Mol. Sci.* **2022**, *23*, 8225.
[21] G. Nelson, M A. Hoon, J. Chandrashekar, Y. Zhang, N J. P. Ryba, C S. Zuker, *Cell* **2001**, *106*, 381.
[22] K K. Yee, S K. Sukumaran, R. Kotha, T A. Gilbertson, R F. Margolskee, *Proc. Natl. Acad. Sci. U S A.* **2011**, *108*, 5431.
[23] E. von Molitor, K. Riedel, M. Krohn, R. Rudolf, M. Hafner, T. Cesetti, *Pflugers. Arch.* **2020**, *472*, 1667.
[24] K. Yasumatsu, T. Ohkuri, R. Yoshida, S. Iwata, R F. Margolskee, Y. Ninomiya, *Acta. Physiol.* **2020**, *230*, e13529.

[25] J. Pan, L. Zhang, X. Shao, J. Huang, *Front. Cell Dev. Biol.* **2020**, *8*, 606.
[26] M. S. Strine, C. B. Wilen, *PLoS Pathog.* **2022**, *18*, e1010318.
[27] M. Ohmoto, T. Yamaguchi, J. Yamashita, A. A. Bachmanov, J. Hirota, I. Matsumoto, *Biosci., Biotechnol., Biochem*. **2013**, *77*, 2154.
[28] J. Yamashita, M. Ohmoto, T. Yamaguchi, I. Matsumoto, J. Hirota, *PLoS One* **2017**, *12*, e0189340.
[29] K. Deckmann, K. Filipski, G. Krasteva-Christ, M. Fronius, M. Althaus, A. Rafiq, T. Papadakis, L. Renno, I. Jurastow, L. Wessels, M. Wolff, B. Schütz, E. Weihe, V. Chubanov, T. Gudermann, J. Klein, T. Bschleipfer, W. Kummer, *Proc. Natl. Acad. Sci. U S A.* **2014**, *111*, 8287.
[30] K. Deckmann, G. Krasteva-Christ, A. Rafiq, C. Herden, J. Wichmann, S. Knauf, C. Nassenstein, C. G. Grevelding, A. Dorresteijn, V. Chubanov, T. Gudermann, T. Bschleipfer, W. Kummer, *Int. Immunopharmacol.* **2015**, *29*, 51.
[31] K. Deckmann, A. Rafiq, C. Erdmann, C. Illig, M. Durschnabel, J. Wess, W. Weidner, T. Bschleipfer, W. Kummer, *FASEB J.* **2018**, *32*, 2903.
[32] C. Kandel, P. Schmidt, A. Perniss, M. Keshavarz, P. Scholz, S. Osterloh, M. Althaus, W. Kummer, K. Deckmann, *Front. Cell Dev. Biol.* **2018**, *6*, 89.
[33] W. Kummer, K. Deckmann, *Curr. Opin. Urol.* **2017**, *27*, 85.
[34] A. Perniss, P. Schmidt, A. Soultanova, T. Papadakis, K. Dahlke, A. Voigt, B. Schütz, W. Kummer, K. Deckmann, *Cell Tissue Res.* **2021**, 21.
[35] K. Deckmann, W. Kummer, *Histochem. Cell Biol.* **2016**, *146*, 673.
[36] D T. Montoro, A L. Haber, M. Biton, V. Vinarsky, B. Lin, S E. Birket, F. Yuan, S. Chen, H. M. Leung, J. Villoria, N. Rogel, G. Burgin, A M. Tsankov, A. Waghray, M. Slyper, J. Waldman, L. Nguyen, D. Dionne, O. Rozenblatt-Rosen, P. R. Tata, H. Mou, M. Shivaraju, H. Bihler, M. Mense, G J. Tearney, S M. Rowe, J F. Engelhardt, A. Regev, J. Rajagopal, *Nature* **2018**, *560*, 319.
[37] M. R. Howitt, Y. G. Cao, M. B. Gologorsky, J. A. Li, A. L. Haber, M. Biton, J. Lang, M. Michaud, A. Regev, W. S. Garrett, *Immunohorizons* **2020**, *4*, 23.
[38] D. D Banik, L. E. Martin, M. Freichel, K. F. Medler, *Proc. Natl. Acad. Sci. U S A.* **2018**, *115*, E772.
[39] S. K. McLaughlin, P. J. McKinnon, R. F. Margolskee, *Nature* **1992**, *357*, 563.
[40] D B. Joseph, G H. Henry, A. Malewska, N S. Iqbal, H M. Ruetten, A E. Turco, L L. Abler, S K. Sandhu, M T. Cadena, V S. Malladi, J C. Reese, R J. Mauck, J C. Gahan, R C. Hutchinson, C G. Roehrborn, L A. Baker, C M. Vezina, D W. Strand, *Prostate* **2020**, *80*, 872.
[41] D. B. Joseph, G. H. Henry, A. Malewska, J. C. Reese, R. J. Mauck, J. C. Gahan, R. C. Hutchinson, V. S. Malladi, C. G. Roehrborn, C. M. Vezina, D. W. Strand, *J. Pathol.* **2021**, *255*, 141.
[42] M I. Hollenhorst, I. Jurastow, R. Nandigama, S. Appenzeller, L. Li, J. Vogel, S. Wiederhold, M. Althaus, M. Empting, J. Altmüller, A K. H. Hirsch, V. Flockerzi, B J. Canning, A.-E. Saliba, G. Krasteva-Christ, *FASEB J.* **2020**, *34*, 316.
[43] T. Li, A. Ihanus, P. Ohukainen, M.-R. Järvelin, J. Kettunen, V.-P. Mäkinen, T. Tynkkynen, M. Ala-Korpela, *Int. J. Epidemiol.* **2022**, *51*, 2022.
[44] G. S. Lund, C. G. L. Wolf, *Biochem. J.* **1925**, *19*, 538.
[45] I. S. Menzies, *Absorption of Intact Oligosaccharide in Health, Disease*, Biochemical Society Transactions, **1974**, *2*, 1042.
[46] L S. Freedman, V. Kipnis, D. Midthune, J. Commins, B. Barrett, V. Sagi-Kiss, S A. Palma-Duran, C S. Johnston, D M. O'Brien, N. Tasevska, *Cancer Epidemiol., Biomarkers Prev.* **2022**, *31*, 1227.
[47] T. Intemann, I. Pigeot, S. De Henauw, G. Eiben, L. Lissner, V. Krogh, K. Deren, D. Molnár, L A. Moreno, P. Russo, A. Siani, I. Sirangelo, M. Tornaritis, T. Veidebaum, V. Pala, *Eur. J. Nutr.* **2019**, *58*, 1247.
[48] A. M. C. P. Joosen, G. G. C. Kuhnle, S. A. Runswick, S. A. Bingham, *Int. J. Obes.* **2008**, *32*, 1736.
[49] C. Luceri, G. Caderni, M. Lodovici, M. T. Spagnesi, C. Monserrat, L. Lancioni, P. Dolara, *Cancer Epidemiol., Biomarkers Prev.* **1996**, *5*, 167.
[50] S. Ramne, N. Gray, S. Hellstrand, L. Brunkwall, S. Enhörning, P. M. Nilsson, G. Engström, M. Orho-Melander, U. Ericson, G. G. C. Kuhnle, E. Sonestedt, *Front. Nutr.* **2020**, *7*, 62.
[51] N. Tasevska, S A. Palma-Duran, V. Sagi-Kiss, J. Commins, B. Barrett, V. Kipnis, D. Midthune, D M. O'Brien, L S. Freedman, *J. Nutr.* **2023**, *153*, 1816.
[52] N. Tasevska, S A. Runswick, A. McTaggart, S A. Bingham, *Cancer Epidemiol., Biomarkers Prev.* **2005**, *14*, 1287.
[53] N. Deane, H. W. Smith, *J. Clin. Invest.* **1955**, *34*, 681.
[54] A. Moncrieff, R. H. Wilkinson, *Acta Paediatr.* **1954**, *43*, 495.
[55] H. Bickel, *J. Pediatr.* **1961**, *59*, 641.
[56] J. A. Owen, I. C. Lewis, *Scott. Med. J.* **1956**, *1*, 231.
[57] R. Santini, E. Perez-Santiago, J. Martinez-de Jesus, C. E. Butterworth, *Am. J. Dig. Dis.* **1957**, *2*, 663.
[58] E. Wimmer, W. Hohenwallner, P. H. Clodi, *Wien Klin Wochenschr* **1978**, *90*, 789.
[59] F. Arrellano-Valdez, M. Urrutia-Osorio, C. Arroyo, E. Soto-Vega, *SpringerPlus* **2014**, *3*, 549.
[60] H. Tanaka, K. Takano, H. Iijima, H. Kubo, N. Maruyama, T. Hashimoto, K. Arakawa, M. Togo, N. Inagaki, K. Kaku, *Adv. Ther.* **2017**, *34*, 436.
[61] R J. Lee, J M. Kofonow, P L. Rosen, A P. Siebert, B. Chen, L. Doghramji, G. Xiong, N D. Adappa, J N. Palmer, D W. Kennedy, J L. Kreindler, R F. Margolskee, N A. Cohen, *J. Clin. Invest.* **2014**, *124*, 1393.
[62] M. Ohmoto, I. Matsumoto, A. Yasuoka, Y. Yoshihara, K. Abe, *Mol. Cell. Neurosci.* **2008**, *38*, 505.
[63] P. Scholz, B. Kalbe, F. Jansen, J. Altmueller, C. Becker, J. Mohrhardt, B. Schreiner, G. Gisselmann, H. Hatt, S. Osterloh, *Chem. Senses* **2016**, *41*, 313.
[64] M. Sigoillot, A. Brockhoff, E. Lescop, N. Poirier, W. Meyerhof, L. Briand, *Appl. Microbiol. Biotechnol.* **2012**, *96*, 1253.
[65] M. Sigoillot, A. Brockhoff, W. Meyerhof, L. Briand, *Appl. Microbiol. Biotechnol.* **2012**, *96*, 619.

